Planar Distance and Velocity Sensor

Jörg Kramer, *Student Member, IEEE,* Peter Seitz, *Member, IEEE,* and Henry Baltes, *Member, IEEE*

***Abstract*— A planar distance and velocity sensor based on a hybrid combination of a light source and a single CMOS photodetector/analog/digital chip is presented. The specific shape of the photodetector calculates a nonlinear geometrical correction purely optically. Hence, electronic data processing is reduced to a minimum, and it can be performed in the analog domain, on the same CMOS chip where the photodetector is placed. Since the (analog) distance and velocity signals are generated simultaneously, the device is particularly useful for time-to-contact measurements.**

I. Introduction

A DISTANCE sensor measures the separation of an object surface from a given reference plane. For various applications, optical systems are preferable to tactile sensors, because they are less likely to damage delicate objects, and optical implementations are more practical for larger working distances and ranges. For distances and ranges of the order of a few tens of millimeters, active triangulation is the most widely used optical measurement method. Triangulation systems interact with the object from two or more different directions. In active devices, at least one of these is employed for structured illumination. Distance information is extracted from the parallax, as described, for example, in [1].

The standard setup of a distance sensor based on active triangulation is shown in Fig. 1. A laser diode or a light-emitting diode (LED) focused somewhere into the measuring volume illuminates a small area of the object surface. Backscattered light is collected by a lens imaging the surface area onto a position-sensitive photodetector (PSP), usually implemented with a lateral-effect photodiode, a so-called position-sensitive device (PSD) [2]. Unfortunately, the relationship between the distance of the object and the position of the light spot on the detector is only linear if the PSP is parallel to the direction of illumination [3]. For conventional triangulation angles between 10° and 20°, this results in an almost grazing incidence of the light on the PSP and a very limited detectable range. All other setups exhibit a distance-dependent magnification which is usually corrected by the data processing electronics.

We integrated the entire detection and processing circuit of a triangulation distance sensor on a single silicon chip covering an area of 1.5 mm × 2.3 mm, fabricated with an industrial CMOS process. The layout of this chip is shown in Fig. 2.

Manuscript received April 18, 1994.

J. Kramer is currently with the Department of Computation and Neural Systems, Division of Biology, California Institute of Technology, Pasadena, CA 91125 USA.

P. Seitz is with the Paul Scherrer Institute Zurich, Badenerstrasse 569, CH–8048 Zurich, Switzerland.

H. Baltes is with the Swiss Federal Institute of Technology, Physical Electronics Laboratory, ETH-Hönggerberg HPT, CH - 8093 Zurich, Switzerland.

IEEE Log Number 9404304.

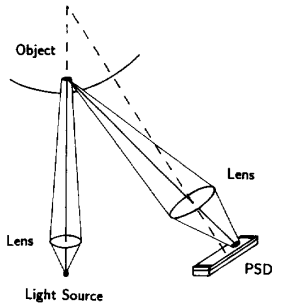

Fig. 1. Standard optical setup of a distance sensor based on active triangulation.

By implementing a nonlinear PSP with a position response correcting the geometrical nonlinearity of the optical setup, it is possible to reduce the electronic signal processing to a minimum using a fully analog circuit. The circuit produces an output signal proportional to the distance between object and sensor. Using a simple analog differentiation circuit, it is straightforward to derive from the distance signal simultaneously a signal proportional to the apparent velocity component of the object in the direction of the sensor. The sensor is also suitable, therefore, for time-to-contact measurements of approaching objects.

II. Nonlinear Correction with Sensor Geometry

Consider a one-dimensional spatial irradiance distribution $I(x)$ in the plane of an optical detector. This irradiance distribution generates a photocurrent [4]

$$L = S \int_{-\infty}^{\infty} I(x) w(x) dx \tag{1}$$

where S denotes the detector's response per incident power (responsivity) and $w(x)$the geometrical width of the photodetector in the y dimension as a function of the x coordinate. This means that the inner product (f, g) of any two positive-definite real functions f and g of a real variable x

$$(f, g) = \int f(x) g(x) dx \tag{2}$$

can be implemented optically. One function is encoded in the light distribution, the other in the detector shape. For a given detector this can be regarded as a weighted average with the detector shape representing the weighting function.

This principle was applied to the fabrication of a PSP with a nonlinear position response, correcting the geometrical nonlinearity in the setup of Fig. 1. This PSP consists of a photodiode with a width $w(x)$ varying along its length

0018–9197/94$04.00 © 1994 IEEE

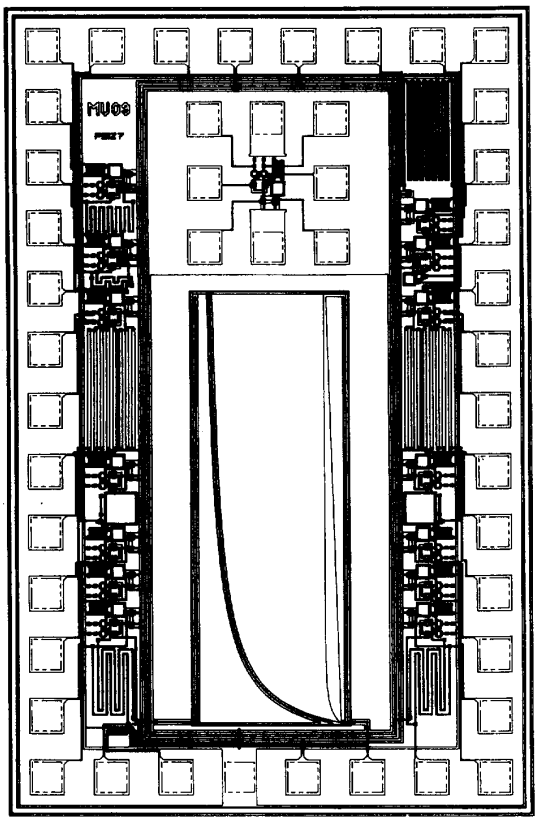

Fig. 2. Layout of the planar distance and velocity sensor integrated with an industrial CMOS process. The total chip size is 1.5 mm × 2.3 mm.

according to the inverse distance correction function $1/x$. An adjoining photodiode is shaped in such a way that the total width of both photodiodes together is constant along their length, providing a means of normalizing the position signal to the incident light power. For this the impinging optical signal to be detected has to form a line of homogeneous irradiance across the detector width. This can be achieved by substituting the imaging lens of the standard setup by a cylindrical lens, or, alternatively, with an astigmatic (possibly diffractive) lens system, capable of imaging a spot onto a thin, homogeneously irradiated line whose length is matched to the width of the PSP.

Considering the ideal case of an infinitesimally thin light line at a position x_0 on the photodetector, the irradiance distribution is given by

$$I(x) = I\delta(x_0) \tag{3}$$

where I denotes the incident power per unit length, and $\delta(x)$ is the Dirac distribution. By substituting (3) into (1) we obtain for the response of the first photodiode

$$L = SIw(x_0) \tag{4}$$

which is proportional to the local width at the position of the light line and to the irradiance. This signal is normalized with the sum of the signals of the two photodiodes, which is independent of position but also proportional to the irradiance. The final output is then proportional to the correction function $w(x_0)$ and independent of the irradiance.

The sensor was laid out to suit the requirements of a compact optical setup with small separations between light source, detecting circuit, and lenses. A measuring distance d ranging from $d_{\min} = 35\,\text{mm}$ to $d_{\max} = 500\,\text{mm}$ was selected. A separation h of the cylindrical lens from the chip of $h = 3\,\text{mm}$ and a distance between the center of the lens and the illuminating beam of $b = 16\,\text{mm}$ were chosen. With the beam perpendicular to the detector plane the resulting triangulation angle is 24° at $d_{\min}$ and 2° at $d_{\max}$. The relationship between d and the corresponding position x along the PSP is given by

$$x = \frac{bh}{d} \tag{5}$$

and the required length l of the PSP is given by

$$l = bh\frac{d_{\max} - d_{\min}}{d_{\max}d_{\min}}. \tag{6}$$

For the specified range a value of $l = 1.2\,\text{mm}$ is obtained. With the chosen maximum width $w_{\max} = 0.35\,\text{mm}$ for the first photodiode PD1, the local width $w(x)$ of PD1 can now be determined according to

$$w(x) = \frac{bhw_{\max}}{xd_{\max} + bh}. \tag{7}$$

III. Electronic Signal Processing

The data processing circuit is shown schematically in Fig. 3. As indicated with a dashed line in this figure, the signal processing is almost completely realized on a single chip. The circuit consists of two branches, the first one processing the signal of the first photodiode (PD1) amplified by a 1:10 current mirror, the second one processing the sum of the signals of both photodiodes. In a standard circuit the position signal would be given by the ratio of the outputs of the two branches but since the realization of a precise and stable analog divider is not simple and would take a lot of chip area, it was decided to avoid it. This can be achieved by performing ac measurements and modulating the light source in such a way that the total light energy reaching the two photodiodes is always the same per given measurement time interval. The light source is turned on at the start of each interval and turned off again when the given amount of optical energy is collected.

Both branches of the circuit first convert the current signal into a voltage (OP1 resp. OP8). For each branch the background voltage produced by the ambient illumination when the light source is turned off is transferred via an unity gain buffer (OP2 resp. OP9) and a gate (Q6p resp. Q7p) to another unity gain buffer. The gate is closed before the light source is turned on at the start of a new measurement cycle. The background signal is then stored on a capacitor (C1 resp. C4) until the gate is opened again when the light source is switched off. This background voltage is subtracted from the continuously measured signal voltage appearing at the output of an unity gain buffer (OP4 resp. OP11) by a differential amplifier (OP5 resp. OP12).

In the first branch the signal modulation is then smoothed out by a lowpass filter (OP6) to output a voltage U_{pos}

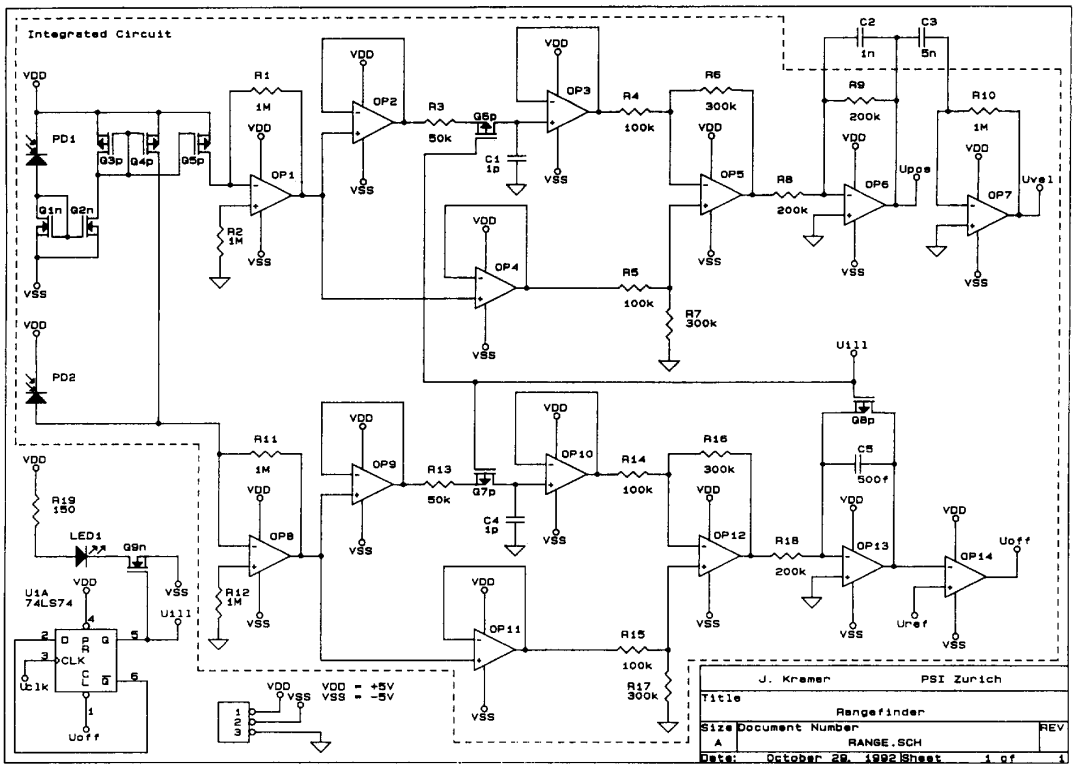

Fig. 3. Complete circuit diagram of the planar distance and velocity sensor. The part of the circuit which is integrated on the chip shown in Fig. 2 is surrounded by a dashed line.

proportional to the measured distance between device and object. Differentiation of U_{pos} (OP7) simultaneously delivers a signal U_{vel} proportional to the speed of the intersection point of the illumination beam and the object surface. In the second branch the signal of the differential amplifier is integrated (OP13) and compared to a reference voltage U_{ref} (OP14). As soon as the integrated signal reaches U_{ref} the output U_{off} of OP14 goes from positive to negative clearing the digital output U_{ill} of the external D flip-flop U1A. The transition of U_{ill} from high to low activates the gates (Q6p and Q7p) in the background voltage paths and the integrator reset gate (Q8p) and turns off the light source. The rising edge of the clock signal U_{clk} fed into U1A initiates the low-to-high transition of U_{ill}, which closes the gates and turns the light source on. U_{clk} determines the measurement rate. The data processing circuit is fully integrated with the exception of the power supply, the clock, the flip-flop, and two capacitors, which would have consumed too much chip area.

IV. Optical Setup

The integrated resistors and capacitors are optimized for a clock frequency of 10 kHz and a maximum power arriving on the detector of 2 μW. Assuming that this maximum power is received from a Lambertian surface with 100% reflectivity at the minimum distance of 35 mm through a lens of 4 mm diameter with a transmission of 50% a maximum power of about 1 mW in the illuminating beam is permitted. Such a moderate level of emitted power can be attained using an LED or a laser diode as the light source. Both types of light emitters are also physically small, and they can easily be intensity modulated.

It is not obvious, though, which of the two light sources is optimum for the present optical triangulation application. Available microoptical components make it possible to generate a "light pencil" using the essentially monochromatic laser diodes, so that a small spot is projected on the object, not much affected by the object's distance. Collimating optics performing near the diffraction limit can generate a spot diameter of less than 25 μm over the whole distance range of 35 to 500 mm. This demands a precise mechanical setup of the laser diode and its collimating optics physically close to it. The small spectral bandwidth of laser diodes is responsible for the speckle pattern generated by the microtopography of the object's diffusely reflecting surface. This speckle pattern is a major limitation of triangulation measurements, as discussed in detail in [5]: The distance measurement uncertainty Δd is governed by the speckle contrast C, the triangulation angle Θ, and the numerical aperture $\sin u$ of the photodetectors' optics, according to the following relationship:

$$\Delta d = \frac{C\lambda}{2\pi \sin u \sin \Theta}. \tag{8}$$

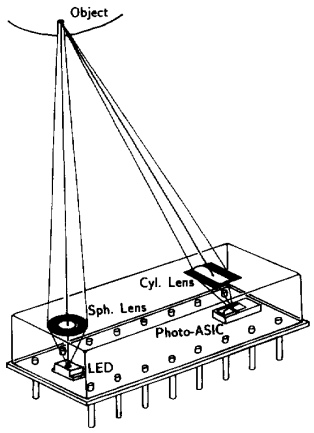

Fig. 4. Schematic diagram of the optical setup of the planar distance and velocity sensor.

Employing an LED as the light source instead of a laser diode reduces the speckle contrast C by at least a factor of three. Unfortunately, an LED as an essentially incoherent light source needs to be focused on the object, leading to distance-dependent broadening of the light spot on the object. The nonlinear relationship (5) between object distance and lateral excursion of the detected, spatially extended light spot causes inaccuracies in the measured object distance. With known geometries and a fixed optical setup, the necessary corrections can be provided by adapting the shape of the photodetector suitably. It is mechanically simpler, therefore, to work with an LED and either to tolerate the measurement inaccuracies caused by defocussing errors, or to include these corrections into a modified sensor shape.

A demonstration device was built by bonding the CMOS chip and an LED onto opposite ends of a 16 pin DIL carrier and integrating the lenses into the cap of the carrier in the form of specially designed, embossed planar Fresnel lenses [6], as shown schematically in Fig. 4. The finished device, without the cap carrying the two planar Fresnel lenses, is shown in the photograph of Fig. 5.

V. Results

The functionality of the circuit and the measurement precision and accuracy of the photosensor were tested by projecting a light stripe (HeNe laser source with a wavelength of 632.8 nm) onto the detector. The output current of PD1 as a function of its local width shows a standard deviation from linearity of 12%, exhibiting an increasing error for smaller photodiode widths. This leads to significant distance measurement inaccuracies of up to 20% of the object distance, due to the erroneously determined lateral position of the light stripe. This rather poor value of the measurement accuracy is due to the crosstalk from the second photodiode (PD2), which is relatively large because the spacing between the two photodiodes is only 15 μm. In order to provide a more accurate correction of the nonlinearity of the optical setup, the shape of the detector would have to be modified to account for the crosstalk, which was not done in the present work. The

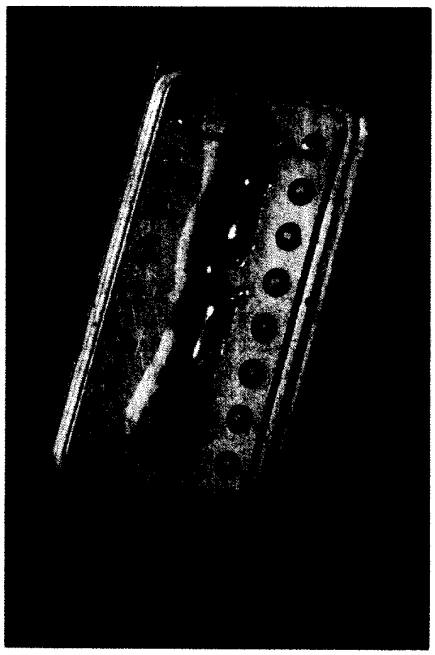

Fig. 5. Photograph of the finished planar distance and velocity sensor in a 16-pin dual-in-line package, without the cap carrying the two lenses.

crosstalk can also be reduced by choosing a larger separation between the photodiodes, by implanting a p^+ channel between the p^- wells to absorb the holes diffusing from one well to the other or by separating the wells either with an n^+ implant or with a positive-biased gate repelling the diffusing holes.

The resolution of the determination of the light stripe position on the detector depends on the light level. For an optical power of 200 nW, the position signal U_{pos} was capable of resolving a displacement of 10 μm near the edge of the PSP covering the close end of the range. This resolution increases to 1 μm towards the edge of the PSP covering the far end of the range. The corresponding resolution in object space decreases from 0.3 mm at a distance of 35 mm to 5 mm at a distance of 500 mm, assuming ideal optical conditions. The relative resolution remains approximately constant, therefore, amounting to 1% of the measured object distance. This represents the ultimate accuracy—at the selected power level of 200 nW—with which the object's distance can be measured, assuming a perfectly corrected photosensor shape and correctly aligned optical components.

No attempt was made to determine precisely the (bandwidth-dependent) resolution and accuracy of the analog velocity signal. In the typical applications we foresee, only a coarse estimate of the velocity signal is of practical interest, sometimes even just a threshold, binary signal, indicating whether the object is moving or not.

The current consumption of the detecting circuit is 250 μA for supply voltages of ± 5 V, corresponding to a dissipated power of 2.5 mW.

As can be seen from Table I, the performance characteristics of the described planar distance sensor is comparable to those

TABLE I
CHARACTERISTICS OF THE PLANAR ANALOG CMOS DISTANCE SENSOR AND OF THREE COMMERCIALLY AVAILABLE DISTANCE SENSORS

	CMOS integrated	T.d.P. Optimess Mini-2	$\mu\epsilon$ LD 1600-100	Laser Components LC-ML-AT-65/50
Range (mm)	35 - 500	150 - 250	35 - 135	40 - 90
Absolute resolution (μm)	300 - 5000	25	100	50
Relative resolution	0.06% - 1.1%	0.025%	0.1%	0.1%
Repetition rate (kHz)	10	10	10	0.1

of commercial devices [7]–[9], which all employ an electronic linearization circuit to generate an output signal proportional to the distance. These devices are much bulkier and consume more power than the described single-chip sensor.

VI. DISCUSSION

A planar distance and velocity sensor was designed and realized on a single 16-pin DIL carrier. Based on active triangulation, the sensor employs a nonlinear position-sensitive photodetector to generate an output signal proportional to the distance of a diffusely reflecting object. The photodetector and the fully analog data processing circuitry are integrated on the same chip using industrial CMOS technology [10]. The sensor delivers the distance and the velocity signals simultaneously, and it is well-suited, therefore, for time-to-contact measurements. The performance of the sensor is comparable to that of commercially available distance sensors, which are much larger, more expensive to produce, and consume more power.

ACKNOWLEDGMENT

The forthcoming help of M. Rossi and H. Schütz (both at the Paul Scherrer Institute in Zürich), in designing and fabricating the planar Fresnel lenses is gratefully acknowledged. We would also like to thank E. Tan (McMaster University, Hamilton, Ontario, Canada) for his support in designing and simulating the employed operational amplifiers.

REFERENCES

[1] J. Kramer, P. Seitz, and H. Baltes, "Inexpensive range camera operating at video speed," *Appl. Opt.*, vol. 32, pp. 2323–2330, 1993.
[2] G. Lucovsky, "Photoeffects in nonuniformly irradiated p-n junctions," *J. Appl. Phys.*, vol. 31, pp. 1088–1095, 1960.
[3] H. Sekii, K. Kitajima, S. Ogata, and K. Imanaka, "Compact and high-resolution displacement sensor using a twin-micro Fresnel lens," in *Tech. Dig. Conf. Lasers and Electro-Optics*, Baltimore, MD, May 12–17, 1991, pp. 462–463.
[4] J. Kramer, P. Seitz, and H. Baltes, "Industrial CMOS technology for the integration of optical metrology systems (photo-ASICs)," *Sensors Actuators A*, vol. A34, pp. 21–30, 1992.
[5] R. G. Dorsch, G. Häusler, and J. M. Herrmann, "Laser triangulation: Fundamental uncertainty in distance measurement," *Appl. Opt.*, vol. 33, pp. 1306–1314, 1994.
[6] R. E. Kunz and M. Rossi, "Phase-matched Fresnel elements," *Opt. Commun.*, vol. 97, pp. 6–10, 1992.
[7] "Optimess Mini-2," Techniques de Pointe SA, Lausanne, Switzerland, Tech. Data Sheet, 1990.
[8] "OptoNCDT Serie 1600," Micro-Epsilon Messtechnik, Ortenburg, Germany, Tech. Data Sheet, Nov. 1989.
[9] "Laser-Abstandsmeß -System LC-ML-AT-X/Y," Laser Components, Gröbenzell, Germany, Tech. Data Sheet, 1991.
[10] J. Kramer, "Photo-ASICs: Integrated optical metrology systems with industrial CMOS technology," Ph.D. dissertation, Swiss Federal Inst. Technol., Zürich (ETHZ), no. 10186, 1993.

Jörg Kramer was born in Zürich, Switzerland. He graduated in physics from the Swiss Federal Institute of Technology (ETH), Zürich, in 1987, and received the M.Sc. degree in applied optics from the Imperial College of Science and Technology, London, England, in 1988.

He is now working toward the Ph.D. degree at the Paul Scherrer Institute in Zürich. His current research interests are in optics and optoelectronics.

Peter Seitz (M '88) was born in Basel, Switzerland. He received the M.Sc. degree in experimental physics in 1980 and the Ph.D. degree in 1984 from the ETH Zürich, Switzerland, working at the Institute for Biomedical Engineering. This work was in the field of computed tomography, specializing in room-temperature semiconducting X-ray detectors and the mathematics of image reconstruction from incomplete projections.

In 1984 he joined Laboratories RCA Ltd. in Zürich, where he worked in the optics and image processing group. In 1987 he transferred to the reorganized laboratory performing high-technology research as part of the Paul Scherrer Institute, where in 1989 he was appointed head of the newly formed image-sensing group. His interests center around solving problems in applied optics and physics, using novel sensors as well as advanced signal- and image-processing techniques.

Henry Baltes (M '81) received the D.Sc. degree from ETH Zürich, Switzerland, in 1971.

In the following years he was on the faculty of the Freie Universität Berlin, the University of Düsseldorf, the University of Waterloo, Ont., Canada, and the Ecole Polytechnique Fédérale Lausanne (EPFL). In 1974 he joined Landis & Gyr Zug Corporation, where he became head of the solid-state device laboratory active in microsensor research. From 1975 to 1982 he taught optics, solid-state physics, and microsensors at EPFL. From 1983 to 1988 he held the Henry Marshall Tory Chair at the University of Alberta, Edmonton, Canada, where he directed a research program in microsensors. As acting President of the Alberta Microelectronic Centre, he was in charge of the establishment of a CMOS fabrication facility. From 1986 to 1988 he also was a director of LSI Logic Corporation of Canada. Since 1988 he has been Professor of Physical Electronics at ETH Zürich and head of ETH's Physical Electronics Laboratory active in silicon microsensors. In 1991 he joined the Board of Directors of Ascom Microelectronics and was appointed Director of the Swiss Federal Priority Program LESIT.

Prof. Baltes is an Associate Editor of *Sensors and Materials* and the *Journal of Micromechanics and Microengineering*. He is a member of the Optical Society of America, the Institute of Physics, the Electrochemical Society, the Swiss Information Technology Society, the Swiss Electrotechnical Association, the Swiss Society for Sensor Technology, and the Swiss Physical Society.